Melting, freezing, and coalescence of gold nanoclusters

Laurent J. Lewis,* Pablo Jensen, and Jean-Louis Barrat
Département de Physique des Matériaux, Université Claude-Bernard Lyon-I, CNRS UMR 5586, 69622 Villeurbanne Cédex, France
(Received 14 March 1997)

We present a detailed molecular-dynamics study of the melting, freezing, and coalescence of gold nanoclusters within the framework of the embedded-atom method. Concerning melting, we find the process first to affect the surface (''premelting''), then to proceed inwards. The curve for the melting temperature vs cluster size is found to agree reasonably well with predictions of phenomenological models based on macroscopic concepts, in spite of the fact that the clusters exhibit polymorphism and structural transitions. Upon quenching, we observe a large hysterisis of the transition temperature, consistent with recent experiments on lead. In contrast, we find macroscopic sintering theories to be totally unable to describe the coalescing behavior of two small clusters. We attribute this failure to the fact that the nanocrystals are faceted, while the sintering theories are formulated for macroscopically smooth crystallites. The time for coalescence from our calculations is predicted to be much longer than expected from the macroscopic theory. This has important consequences for the morphology of cluster-assembled materials.
[S0163-1829(97)07628-5]

I. INTRODUCTION

Nanometer-size particles, or clusters, have received much attention recently.[1] From a fundamental point of view, it is of interest to understand how the properties of nanoparticles are affected by their size, and in particular how the behavior of the bulk material is approached. The field has received considerable impetus from speculations about possible technological applications of nanoparticles in optoelectronic devices. Computer simulation methods, and in particular molecular dynamics (MD), have become a favorite tool for investigating the physics of nanoparticles theoretically. Indeed, with present-day computers, detailed simulations of clusters containing several thousand atoms are easily feasible using empirical potential models.[2] More accurate simulations using *ab initio* interactions are possible for particles containing up to a few tens of atoms, and have indeed been used to study small semiconductor clusters.[3]

In this paper, we use MD simulations to address two issues. First, we investigate the influence of size on the melting and freezing of gold nanoparticles. Second, we examine the coalescence of two gold nanoparticles, both of identical size and nonidentical size. We focus here on gold because it has been the object of several experimental studies,[4,5] and also because semiempirical, many-body potentials are available for this material. The first question has already been addressed by several authors using a variety of approaches, experimental and theoretical.[5–9] We take it here as a preliminary step toward the second stage of our study, namely coalescence. Understanding coalescence is of primary importance for understanding the structure of cluster-assembled materials. These materials can be grown by the low-energy deposition of preformed clusters containing hundreds or thousands of atoms on a surface.[10] The structure of the resulting films depends critically on the diffusion properties of the deposited clusters,[11,12] as well as on their sintering properties. On the basis of thermodynamics, it is evident that clusters deposited on a surface will tend to coalesce and form larger drops. The kinetics of this process, which is determinant for understanding the actual structure of the film, is, however, not known in detail.

Concerning melting, we find the clusters to exhibit premelting prior to the transition. The melting temperature vs size curve is found to agree reasonably well with predictions of phenomenological models based on macroscopic concepts, despite the fact that the clusters exhibit a rather complex structure—polymorphism and structural transitions. Upon quenching, we observe a large hysterisis of the transition temperature. In contrast, we find macroscopic sintering theories to be totally unable to describe the coalescing behavior of two small clusters. We attribute this failure to the fact that the nanocrystals are faceted, while the sintering theories assume macroscopically smooth crystallites. We predict the time for coalescence to be much longer than expected from the macroscopic theories. This will have important consequences for the morphology of cluster-assembled materials. Here we consider the coalescence of unsupported clusters, i.e., in vacuum rather than on a substrate. Evidently, an important role of the substrate in the actual coalescence of supported clusters is to ensure thermalization. In the constant-temperature MD simulations reported below, thermalization is taken care of by coupling the system to a ''thermostat.''[13] We therefore expect the coalescence events studied here to be relevant to supported clusters in the case where they are loosely bound to the substrate, e.g., gold clusters on a graphite substrate.

The paper is organized as follows. The computational details are described in Sec. II. The melting/freezing transition is described and analyzed in Sec. III. Coalescence of two unsupported clusters is decribed in Sec. IV, and Sec. V summarizes our main conclusions.

II. COMPUTATIONAL DETAILS

A. MD simulations

In order to be able to simulate clusters containing more than several hundred particles, as noted above, it is necessary

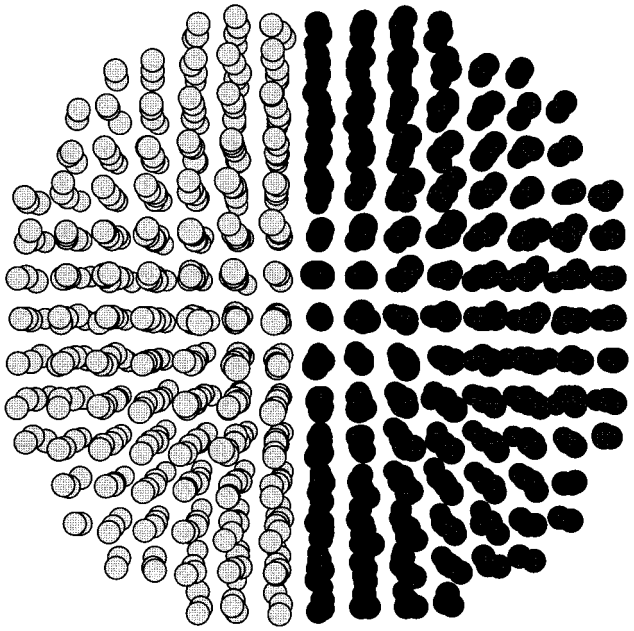

FIG. 1. Structure of the 1055-atom Au cluster in the fcc structure, i.e., before melting and resolidifying, at 300 K. The two halves of the cluster are represented with different colors in order to facilitate visualization of the diffusion processes.

to resort to an empirical description of the interatomic forces. Here we chose to employ the embedded-atom method (EAM),[14] an n-body potential with proven ability to model reliably various static and dynamic properties of transition and noble metals, in either bulk or surface configurations.[15] The model is ''semiempirical'' in the sense that it approaches the total-energy problem from a local-electron-density viewpoint, but using a functional form with parameters obtained from experiment (equilibrium lattice constant, sublimation energy, bulk modulus, elastic constants, etc.).

In the case of gold, EAM gives an excellent description of jump diffusion on the (100) surface (the activation energy is predicted to be 0.64 eV compared to 0.62 eV from first principles),[16] but does not do as well on the (111) surface, where the barrier is very low (0.02 vs 0.20 eV).[16] The melting temperature for bulk Au is predicted by EAM to be 1090 K. This does not agree well with the experimental value of 1338 K. Thus, while we expect the model to give a qualitatively correct description of the nanoclusters, we also expect significant differences to show up in the numerical values of the calculated properties. One interesting advantage of EAM (and similar models) vs more generic models such as the Lennard-Jones model, however, is that the n-body formalism gives a much better description of cohesion in nonequilibrium situations, as is the case on a surface at finite temperature. Thus, for instance, while desorption of atoms on a Lennard-Jones surface is unphysically large, it occurs very rarely on a EAM surface. Hence, in spite of the quantitative limitations of the EAM, we expect the model to provide a qualitatively correct description of the system.

The MD calculations were performed using a parallel version of program groF, a general-purpose MD code for bulk and surfaces developed by one of the authors (L.J.L.), optimized to run on the Convex of the PSMN/ENS.[17] The program employs a predictor-corrector algorithm to integrate the equations of motion, and provides the option to do extended-system simulations (constant temperature and/or constant pressure). In all the simulations reported here, we used a time step of 2.5 fs; this is a fairly small value, which we judged necessary in order to ensure proper stability of the trajectories during the very long runs needed to study coalescence (up to 10 ns, i.e., four million steps).

B. Cluster preparation

The clusters used to initiate the melt-and-freeze runs were prepared as follows: Starting with a large block of face-centered-cubic Au, ''spherical'' clusters were carved out such that the center of mass coincides exactly with an atom. Of course, the clusters cannot be perfectly spherical and will, even in their ground state, exhibit facets. A 1055-atom cluster is shown in Fig. 1. (In order to better follow diffusion processes, the two halves of the cluster are colored differently.) We did not consider using other cluster geometries, such as icosahedral, octahedral, or Wulff polyhedral.

Clusters of eight different sizes were considered, from 135 to 3997 atoms, as indicated in Table I, thus spanning a fairly wide range of melting temperatures (see Sec. III). It should be noted that small clusters can undergo several structural transitions as a function of temperature (below melting), and therefore constitute an object of study in their own right. We actually observed many such transitions in our smaller clusters, but this is beyond the scope of the present study.

After equilibration at low temperature, the clusters were subjected to a melt-and-quench cycle in order to identify the melting temperature and to force the clusters into their ground state. (For the reasons mentioned above only the larger clusters—767 atoms and beyond—were resolidified after melting). Upon approaching the transition from either side, the temperature was changed in steps of 25–100 K. At each temperature, the system was first fully equilibrated before running to accumulate statistics. Typically, runs ranged from 100 to 250 ps, depending on the ''distance'' from the transition, which could be anticipated from the behavior of the potential energy. The melt-and-freeze simulations were carried out in the microcanonical ensemble.

III. MELTING AND FREEZING

A. Total energies

There are several ways of proceeding for identifying the melting and freezing transitions. The simplest is perhaps to

TABLE I. Melting temperature of the various clusters considered in the present study as a function of their radius just before melting, R (given, in terms of the radius of gyration R_g by $R=\sqrt{5/3}R_g$).

N	R (Å)	T_m
135	8.08	530
321	10.89	700
531	12.92	750
767	14.72	775
1055	16.37	835
1505	18.50	865
2093	20.68	900
3997	25.62	930

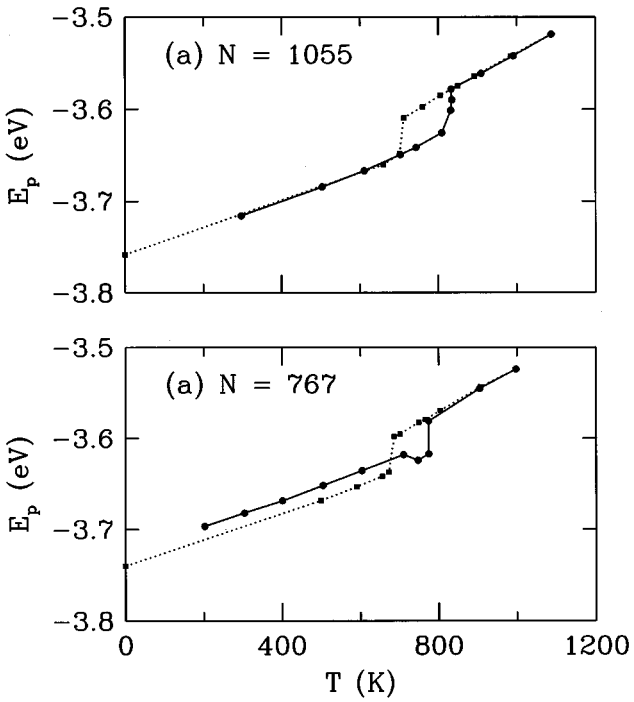

FIG. 2. Potential energy (per atom) as a function of temperature for (a) the 1055-atom cluster and (b) the 767-atom cluster; full and dotted curves correspond to heating and cooling, respectively.

examine the variations of potential energy with temperature. This is done in Fig. 2(a) for the 1055-atom cluster. The ''as-made'' fcc cluster was first equilibrated at 300 K, then heated up slowly until it melted. The melting transition is clearly identifiable by the large upward jump in energy at a temperature of about 835 K; on either side of the transition, the energy varies smoothly, almost linearly with temperature. Very near the transition, the system becomes unstable, and the data points are characteristic of a transient state. Upon cooling from the highest temperature, the system undergoes a sharp liquid-solid transition in spite of a rather strong hysterisis. Clearly, the new solid phase, as far as energy is concerned, is equivalent to the initial one, though, as we will see below, there are some structural differences.

It is much easier for a cluster to go from an ordered state to a disordered state than the opposite, i.e., in the present context, to melt than to freeze during the finite time covered during the simulations. This explains, in part, the hysteresis we observe in the melt-and-quench cycle, and also indicates that the melting temperature is probably much closer to the thermodynamic transition point than the freezing temperature. However, hysteresis in the melting/freezing transition is expected theoretically,[18] and has also been reported experimentally in the case of lead.[19]

In Fig. 2(b) we show the potential energy for the 767-atom cluster. This system exhibits interesting behavior. First, upon heating (solid line), we see that the cluster undergoes a solid-solid transition (of the type mentioned above) to a lower-energy phase (which we have not analyzed in detail), at a temperature of about 710 K, then melts at about 775 K. Upon cooling, freezing takes place at about 680 K, but now to a state that lies somewhat lower in energy than the initial phase—likely the same as that which appeared just below melting, as can be inferred from their comparable energies.

The structure of the low-temperature, resolidified clusters is discussed in more detail below; they differ from the initial, low-temperature, fcc clusters in that large facets are now present. Because of finite-time limitations in the MD simulations, the transition to the ground-state structure is, however, incomplete: while facets develop, the melt-and-quenched clusters are ''packed'' with defects so that, in effect, their energies lie above those of the corresponding fcc clusters for large enough sizes (1505 and beyond).

B. Dynamics and density distributions

Melting and freezing of the clusters can also be quantified in terms of diffusion, as is often done for the corresponding bulk transitions. It is evidently most appropriate, in the case of a cluster, to examine diffusion as a function of distance from the surface. Thus we may define radial bins about the center of mass and calculate, for an average atom within each bin, the mean-square displacement.

In order to define those bins in a physically-meaningful manner, we introduce the density distribution function $N(r)$, where $N(r)dr$ is the number of atoms within a shell of thickness dr at r from the atom at the center of mass of the cluster. We show this quantity at five different temperatures for the 1055-atom cluster in Fig. 3: 297, 703, 809, and 835 upon heating, and 701 upon cooling, averaged over thousands of independent configurations. The results of runs 703 (heating) and 701 (cooling) are superimposed on the same graph so as to display the similarities and differences between the two structures.

From Fig. 3 we see that $N(r)$ for the solid phases of the cluster displays a structure typical of a crystal at finite temperature, i.e., an elaborate series of well-defined peaks broadened by thermal agitation. This is of course particularly true of the inner shells, where the structure is more bulklike. The outer shells, in contrast, feel strongly the influence of the surface, even more so that the temperature is high. This is in fact very reminiscent of corresponding situation in the case of infinite surfaces.

Upon melting, just like a bulk crystal does, $N(r)$ exhibits a behavior similar to that of an ordinary, bulk liquid, i.e., a series of peaks that merges into a featureless continuum at large distances (835 K in Fig. 3). In particular, small peaks merge and the minimum between the first- and second-neighbor peak is filled up, indicating that diffusion is actively taking place.

It is easy to see from Fig. 3 at 835 K that the liquid cluster consists of concentric shells of atoms of thickness roughly equal to the hard-sphere diameter, i.e., about 2.2–2.4 Å here: the atoms are ''rolling'' on top of one another in such a way that the inherent packing arrangement dictated by the central atom is preserved. It is therefore natural to examine diffusion as a function of the radial position of the shell. This is done in Fig. 4, where we plot the mean-square displacements $r^2(t)$ versus time for the same four temperatures as in Fig. 3. Of course, intershell diffusion is also taking place, so in fact an atom will sample a region of radial space that extends beyond its own bin. Here, for a given bin, we average over all atoms that belonged to that bin at $t=0$. In the high-T limit, for a long enough averaging time, all particles will sample evenly the whole cluster.

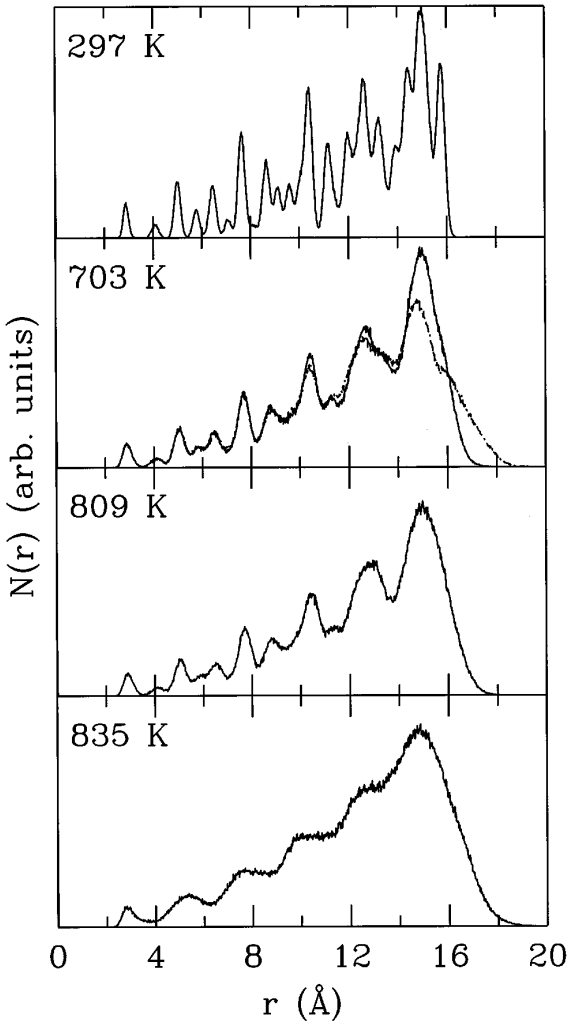

FIG. 3. Density distribution $N(r)$ for the 1055-atom cluster at four different temperatures, as indicated. At $T=703$ K, we show the results for both the initial fcc cluster (full line) and the resolidified cluster (701 K, dashed line). The cluster at 835 K, evidently, is molten.

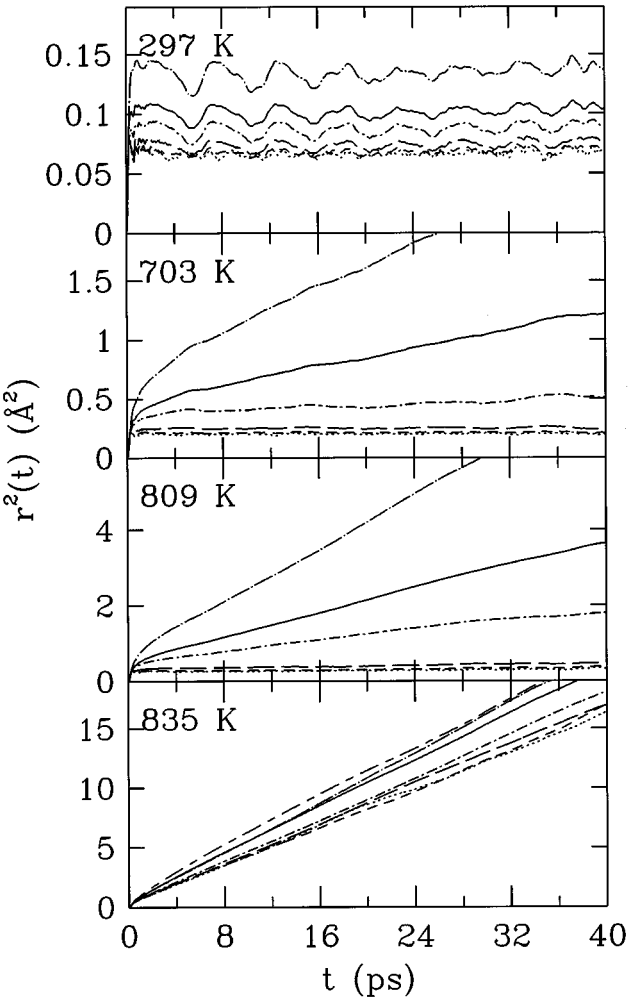

FIG. 4. Mean-square displacements for the 1055-atom cluster at four different temperatures, as indicated, for a series of concentric shells as discussed in the text; the full line, at each temperature, corresponds to the average (over all particles) mean-square displacement.

The mean-square displacements at very low temperatures exhibit a behavior which is typical of a cold crystal with a surface: All shells possess a vanishing diffusion constant (as far as we can tell on the timescale covered by the simulations, viz. $\sim$100 ps) and the amplitude of the oscillations of the atoms about their equilibrium positions increases upon going from the core to the surface, here by a factor of roughly 2.

At 703 K, now, we see that surface diffusion is taking place (this was already visible at somewhat lower temperatures not shown in Fig. 4), but affects only the outer shell. In fact, the corresponding distribution function reveals that the outer-shell peak has lost most of its crystalline character and possesses a rather well-defined liquidlike structure. At 809 K, $N(r)$ is even more liquidlike at the surface, and in fact the two outer shells now possess nonzero diffusion constants. The core of the cluster, however, remains crystalline. This behavior, of course, is related to surface ''premelting,'' as observed in the case of large crystals—see, e.g., Refs. 7 and 20. At the next temperature shown, finally, 835 K, i.e., right above the melting transition, the system is completely liquid, as can be inferred from the shape of $N(r)$ but also from the nonzero, large, and almost identical, diffusion constants for all shells.

C. Atomic structure

An interesting characteristic of the hot-solid phase of the cluster is that even though the *surface* is definitely liquid—cf. Fig. 4 at 809 K—it exhibits very well-defined facets, i.e., the cluster is *not* spherical. This can be seen clearly in Fig. 5(a) for the 1055-atom cluster at 809 K—about 25 K below melting—and even more so in Fig. 5(b) at the same temperature, but after melting and freezing. Such facets reflect the surface anisotropy induced by the core of the cluster, which remains solid at this temperature.

Even more striking, however, is the fact that *even in the molten state*, the instantaneous shape of the cluster deviates markedly from spherical. We see an example of this in Fig.

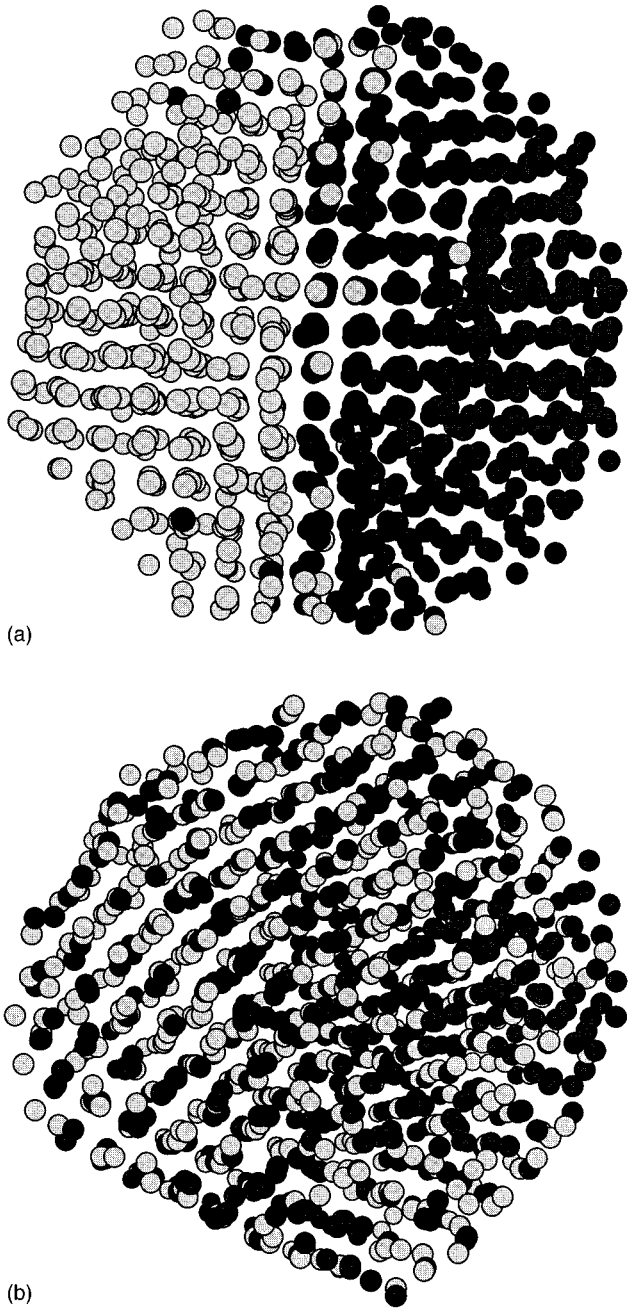

FIG. 5. Structure of the 1055-atom cluster (a) at 809 K, before melting (i.e., in the fcc structure) and (b) at 805 K, after melting and resolidifying.

6, again for the 1055-atom cluster, at a temperature of about 800 K, i.e., 90° *above* freezing. The surface of the cluster exhibits flattened regions, which evidently are reminiscent of the facets that form on the surface of solid, crystalline clusters. It is not clear whether this anisotropic shape reflects some transient crystalline order in the vicinity of the surface, i.e., some precursor fluctuations of the nearby transition, or whether it is related to the deformation modes (breathing) of the liquid cluster, or a combination of both. We have attempted to assess the existence of facets in a more quantitative manner, but the quality of statistics, coupled to significant thermal agitation at such high temperatures, is such that it is difficult to draw unambiguous conclusions.

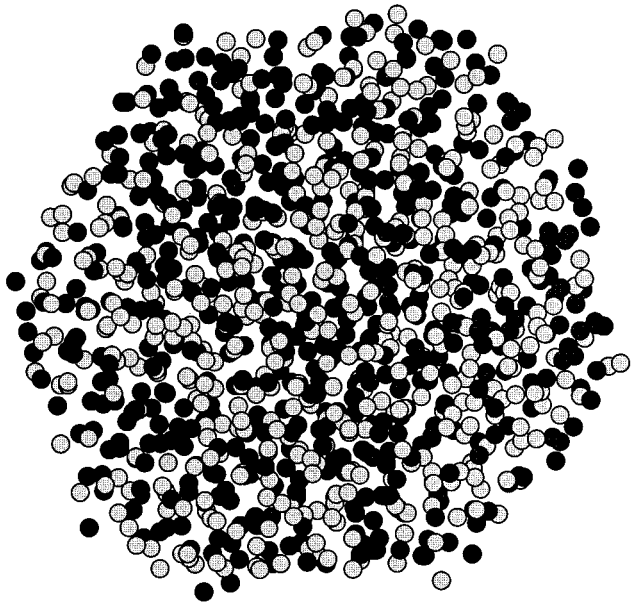

FIG. 6. Structure of the 1055-atom cluster at 800 K during the quench process (i.e., in the liquid phase).

In any case, the fact that both the hot solid and the liquid (at least close to the transition temperature) display anisotropic cluster shapes is an important result. It will have important consequences for the coalescence of clusters. Indeed, diffusion on a facet is very different from diffusion in a (quasi)spherical liquid overlayer. Far away from the edges of the facet, barriers for diffusion are very similar to those found in a flat, infinite, liquid overlayer, i.e., atoms do not ''feel'' the curvature of the cluster. At the edges between two facets, further, the barriers can also be very different and oppose diffusion.[21] Thus, quite generally, diffusion on a faceted cluster is expected to be significantly slower than on a spherical cluster.

Upon cooling, as discussed earlier, a freezing transition takes place. In Fig. 3 we compare the distribution $N(r)$ for the initial cluster at 703 K with that of the resolidified cluster at (approximately) the same temperature. It is clear, from this quantity, that the two clusters have quite similar structures except in their outer shells, because of the presence, in the re-solidified cluster, of extensive facets [such as those seen in Fig. 5(b)].

D. Melting curve

The melting curve—i.e., the variation of melting temperature with cluster size (defined as $D=2R=2\sqrt{5/3}R_g$, where R_g is the radius of gyration of the cluster before melting), is displayed in Fig. 7. We also show, on this graph, the results from a simple thermodynamic theory based solely on the differences in surface energies of clusters of different sizes, assuming the clusters are spherical:[5,22]

$$\frac{T(D)-T_\infty}{T_\infty}=-\frac{4}{\rho_S L D}[\gamma_S-\gamma_L(\rho_S/\rho_L)^{2/3}], \qquad (1)$$

where $T(D)$ is the melting temperature for a cluster of diameter D, T_∞ is the bulk melting temperature (1090 K for the present model), ρ_S the specific mass of the solid phase

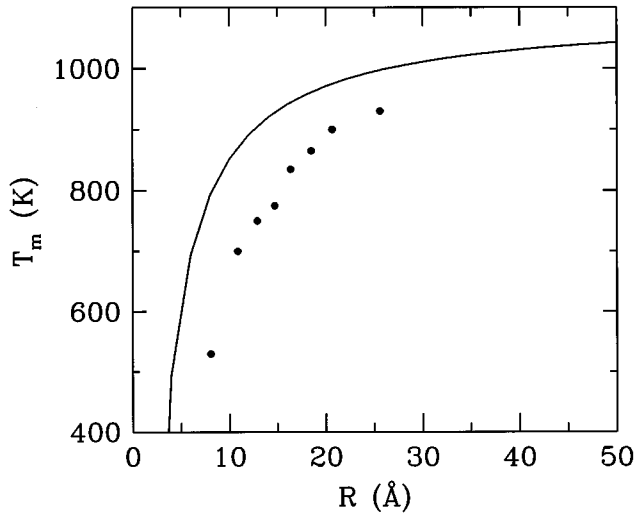

FIG. 7. Melting temperature as a function of cluster radius. The points indicate the results of the simulations, while the solid line shows the predictions of the simple thermodynamic model discussed in the text.

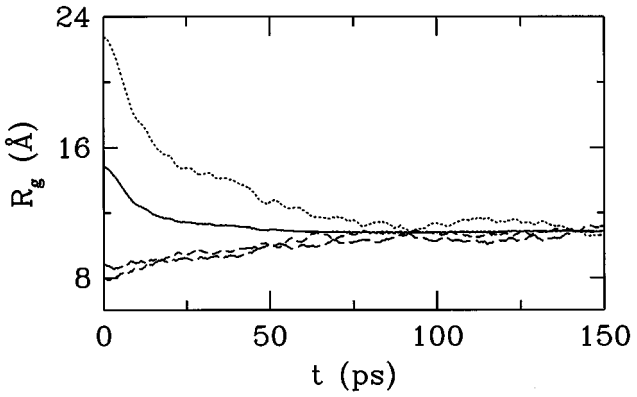

FIG. 8. Radii of gyration for the coalescence of two 321-atom liquid clusters. The dashed lines correspond to the x and y components, while the dotted line is along z; the full line is the overall radius of gyration.

(19 000 kg/m^3), ρ_L the specific mass of the liquid phase (17 280 kg/m^3), γ_S the surface energy of the solid phase (0.9 J/m^2), γ_L the surface energy of the liquid phase (0.74 J/m^2), and L the heat of fusion (53 800 J/kg). Note that, for consistency, all numerical values refer to the results from EAM simulations with parameters appropriate to gold, rather than to experimental data for the real material. We see that, despite the simplicity of the model, the agreement is reasonable, comparable in fact to that with experimental data;[5] just as is observed in experiment, Eq. (1) systematically underestimates the deviation of the melting temperature with respect to the bulk.

IV. COALESCENCE

As a first step toward understanding the aggregation of clusters diffusing on surfaces, and the subsequent pattern formation,[11] we studied the coalescence of pairs of free-standing (nonsupported) clusters. As discussed in Sec. I, this would correspond to the coalescence of clusters on a surface with which they are only loosely bound (e.g., gold on graphite). Three different cases were considered: coalescence of a liquid cluster with another liquid, of a liquid and a solid, and of two solids. The sintering of two single-crystal Cu nanoparticles was examined in Ref. 23. It is possible to study the coalescence of clusters in various thermodynamic states because, as we have just seen, the melting temperature depends on cluster size. Thus, at a given temperature, the state of a cluster can be selected simply by selecting its size.

Here we chose to investigate coalescence at a temperature of 800 K, which is roughly in the middle of the range of melting temperatures for the single clusters reported above (cf. Fig. 7), and therefore allows many possible situations to be examined. We note that once coalescence is finished (or partly finished), the melting temperature of the resulting cluster will be different from that of the original clusters. Thus, for instance, two small liquid clusters will result in a larger cluster which is also a liquid, while two larger liquids would coalesce into a solid. (We have not studied the latter situation).

In order to simulate the process, we use, as starting point configuration, two fully equilibrated clusters from the runs described in Sec. III, i.e., we retain, for each cluster, both the positions and the velocities. The two clusters are placed in contact with one another (along the z axis), i.e., at a distance of approach roughly equal to the nearest-neighbor distance for gold (2.89 Å). We also ensure that the initial angular momentum vanishes. For like clusters, we use configurations from different points in time, and rotate them with respect to one another by an angle which is chosen at random; indeed, it is expected that coalescence will proceed differently if two facets are in contact than if a facet of one cluster is in contact with a vertex of the other.

A. Liquid-liquid

We present, first, results for two small liquid clusters—321+321 atoms. From Fig. 7, we know that the resulting cluster will also be in a liquid state. We show in Fig. 8 the evolution in time of the radii of gyration of the coalescing clusters $R_{g\alpha}$ and R_g, where $\alpha=x,y,z$, $R_g=\sqrt{R_{gx}^2+R_{gy}^2+R_{gz}^2}$, and $R_{g\alpha}=(1/N)\Sigma_{i=1}^{N}(\alpha_i^2-\alpha_{cm}^2)$; α_{cm} is the α coordinate of the center of mass of the cluster, and N is the total number of particles. It is clear from this figure that the two small clusters rapidly coalesce into a single, essentially spherical, cluster: all three radii of gyration converge to the overall average on a time scale of about 75 ps. A ball model of the system in its initial configuration and at 75 ps is presented in Fig. 9. We have colored the two initial clusters differently so as to better visualize the process. It is interesting to note that coalescence into a spherical cluster proceeds by the deformation of the two clusters in such a way as to optimize the contact surface, i.e., *without* interdiffusion of one cluster into—or onto—the other. Thus the coalescence of two liquid clusters is essentially a collective phenomenon, involving hydrodynamic flow driven by surface tension forces. Of course, on longer time scales, since the cluster is liquid, diffusion takes over and results in the mixing of the two initial clusters.

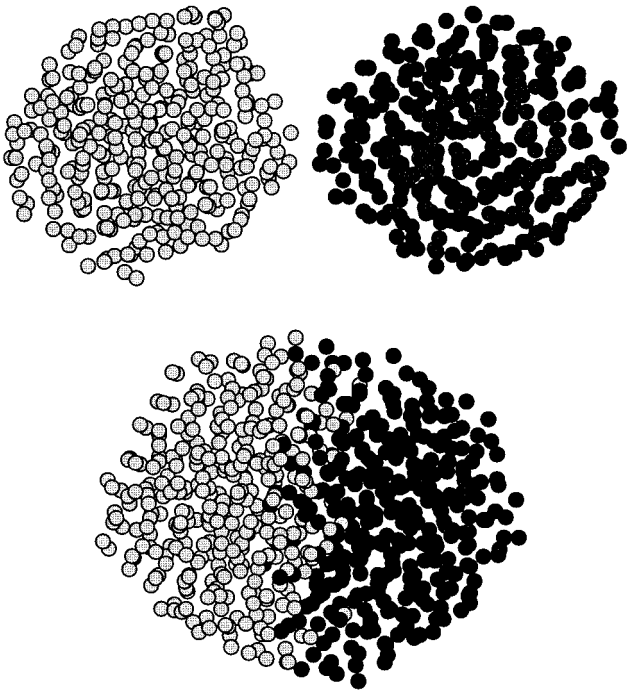

FIG. 9. Coalescence of two 321-atom liquid clusters. Top: initial configuration; bottom: after 75 ps.

B. Liquid-solid

We now examine the coalescence of a liquid cluster with a solid one taking, as an illustration, the case 767+1505. The process in this case is expected to be much slower than 321 +321, and the dynamics, therefore, was followed over a much longer time span of 10 ns. We plot in Fig. 10(a) the radii of gyration for this system. This reveals that coalescence proceeds in two stages: First, maximizing the contact surface (against overall volume), an extremely rapid approach of the two clusters is observed, taking place on a time scale of about 100 ps. This, in fact, corresponds quite closely to the time for coalescence of two liquid clusters, as we have seen above. The cluster, at this point, is far from spherical, but is nevertheless smooth, possessing a faceted ovoidal shape. This can be seen in Fig. 11, where we show the state of the cluster at a time of 1 ns after the beginning of the coalescence. The initial stage of coalescence (sintering) has been studied in some detail in Ref. 23 for two solid Cu clusters.

This rapid approach is followed by an extremely slow ''sphericization'' of the system, driven by surface diffusion. This can in fact be inferred from Fig. 10(a). However, because the system can reorient in space, the radii of gyration, which are defined with respect to a fixed reference frame, do not provide a reliable characterization of the shape of the cluster. In order to circumvent this difficulty, it is best to consider, instead, the three principal moments of inertia; we plot, in Fig. 10(b), the ratio of the smallest to the largest as a function of time. This is in effect a measure of the ''aspect ratio'' of the coalescing cluster; it should be noted that, by definition, this quantity is always less than unity. Also, there are necessarily fluctuations in it that are related to the modes of vibration of the cluster. Figure 10(b) reveals that, indeed, *modulo* some fluctuations, the cluster exhibits a tendency to adopt a more spherical shape.

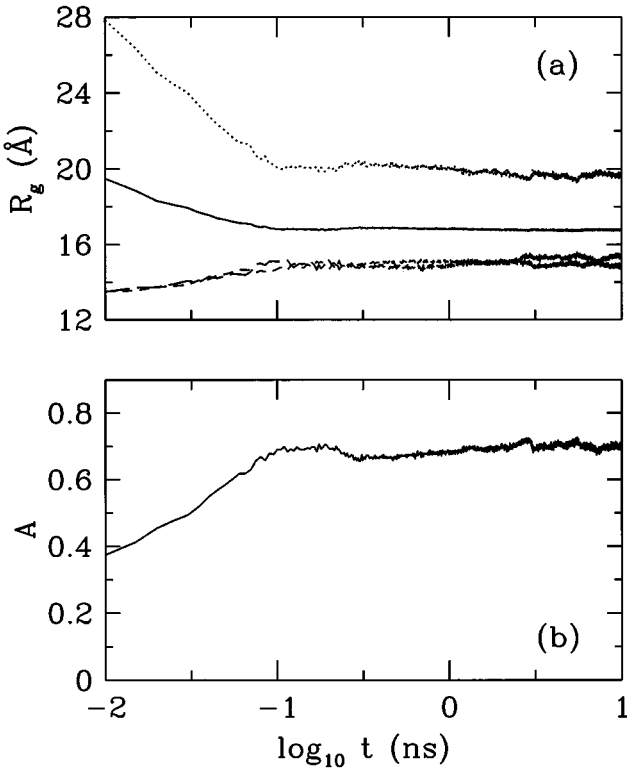

FIG. 10. (a) Radii of gyration and (b) aspect ratio, as defined in the text, vs time, for the coalescence of a 767-atom liquid cluster with a 1505-atom solid cluster.

The time scale for the slow sphericization process is difficult to estimate from Fig. 10, but it would appear to be of the order of a few hundred ns or more. In any case, this number is very substantially larger than one would expect on the basis of phenomenological theories of the coalescence of two soft spheres.[24] Indeed, macroscopic theories of sintering via surface diffusion[24] predict a coalescence time $\tau_c = k_B T R^4/(C D_s \gamma a^4)$, where D_s is the surface diffusion constant, a the atomic size, γ the surface energy, R the initial cluster radius, and C a numerical constant ($C=25$ according to Ref. 24); taking $D_s \sim 5\times 10^{-10}$ m^2 s^{-1} (see Fig. 4), $R=30$ Å, $\gamma \approx 1$ J m^{-2}, and $a=3$ Å, this yields a coalescence time τ_c of the order of 40 ns.

The same theories, in addition, make definite predictions on the evolution of the shape of the system with time. In particular, in the tangent-sphere model, the evolution of the ratio x/R, where x is the radius of the interfacial neck, computed numerically,[24] is found to vary as $x/R \sim (t/\tau_c)^{1/6}$ for values of x/R smaller than the limiting value $2^{1/3}$. In Fig. 12, we compare the prediction of this simple model (full line) with the results of the present simulations (averaged over several different runs, including solid-solid coalescence—see below). There is evidently no possible agreement between model and simulations. While the model predicts a uniform behavior over a wide range of time scales, we observe a very rapid growth at short times followed by an extremely slow increase at long times. The rapid changes we see at short times are due to elastic and plastic deformations not taken into account in the numerical model; at long times, on the other hand, the presence of facets slows down the diffusion, while the model assumes the cluster to be perfectly spherical.

FIG. 11. Configuration of the 767+1505 liquid-solid system at three different times: 0, 1 ns, and 10 ns (top to bottom).

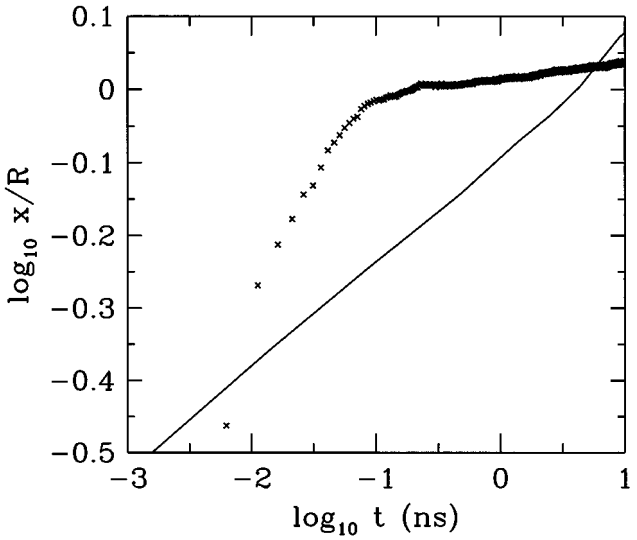

FIG. 12. Evolution in time of the ratio of the neck radius, x, to the cluster radius R. The full line represents the numerical solution obtained by Nichols (Ref. 24), while the crosses are the results of the present simulations.

As already noted above, our results are clearly not compatible with a coalescence time τ_c of 40 ns; the actual value is evidently much larger, by at least one or two orders of magnitude.

The much longer coalescence time we observe, again, is a consequence of the presence of facets on the initial clusters, which persist (and rearrange) during coalescence. The facets can be seen in the initial and intermediate configurations of the system in Fig. 11; the final configuration of Fig. 11 shows that the cluster is more spherical (at least from this viewpoint), and that new facets are forming. As mentioned earlier, facets seriously limit the rate of diffusion that is necessary to sphericize the cluster. Since a facet is flat, an atom diffusing on it does not ''feel'' the curvature of the cluster, and therefore behaves as if it was on a flat, infinite surface—except when approaching edges. We have not examined this in detail for the case of gold, but in the case of aluminum, the diffusion barriers at edges are found to be often larger than on surfaces; for Al, e.g., diffusion from (100) to other facets is *not* observed until temperatures very close to melting,[21] and is therefore not a favorable process. That diffusion is slow on our clusters can in fact be seen from Fig. 11: even after 10 ns, at a temperature which is only about 200° below melting for a cluster of this size, only very few atoms have managed to diffuse a significant distance away from the contact region.

We have not analyzed in detail the structure (and its evolution in time) of the cluster. However, it is clear from Fig. 11 that already at 1 ns, the system is completely solid, i.e., the initially liquid cluster has solidified upon coalescing with the larger solid cluster. Visual inspection of the configurations indicates that the time scale for solidification is roughly the same as that for the initial approach—about 100 ps.

C. Solid-solid

Finally, we have also examined the coalescence of two solid, 1055-atom clusters. We give in Figs. 13(a) and 13(b) the evolution in time of the radii of gyration and of the aspect ratio, as defined above, respectively. In Fig. 14 we show the initial state of the system as well as at times of 1 and 10 ns.

The behavior of the system in this case is analogous to that found for the liquid-solid case (passed the initial approach). One apparent difference, however, is that coalescence seems to proceed *faster* here than it did for the liquid-solid case; this can be seen upon comparing the aspect ratios, Figs. 13(b) and 10(b). Note that since the present system is larger, the diffusion should be relatively slower, since the distance in temperature to the melting point is larger, i.e., sphericization should proceed more *slowly*.

Of course, we cannot draw general conclusions based on these two particular examples, and it is certainly the case that the coalescence of a liquid and a solid proceeds faster, in general, than the coalescence of two solids. (We have observed such cases). The particular behavior we observe here is likely related to the internal structure of the cluster: Judg-

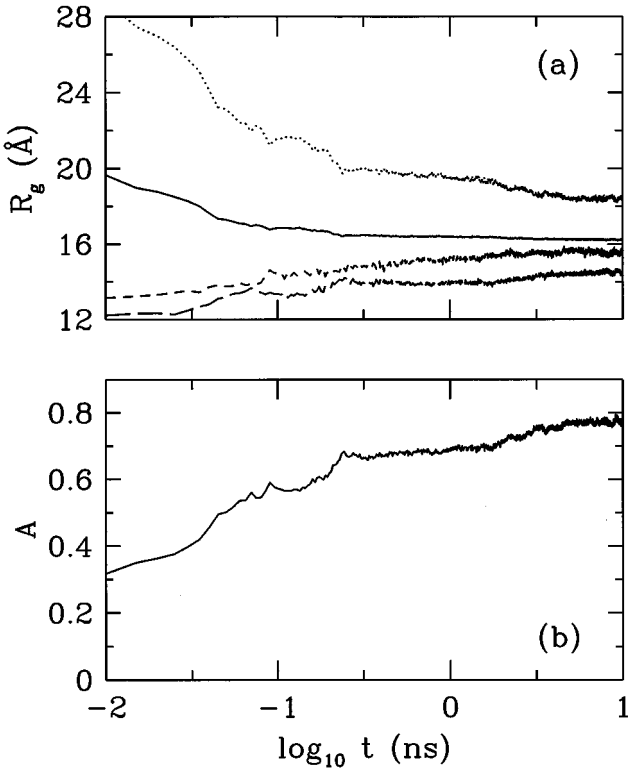

FIG. 13. (a) Radii of gyration and (b) aspect ratio, vs time, for the coalescence of two 1055-atom solid clusters.

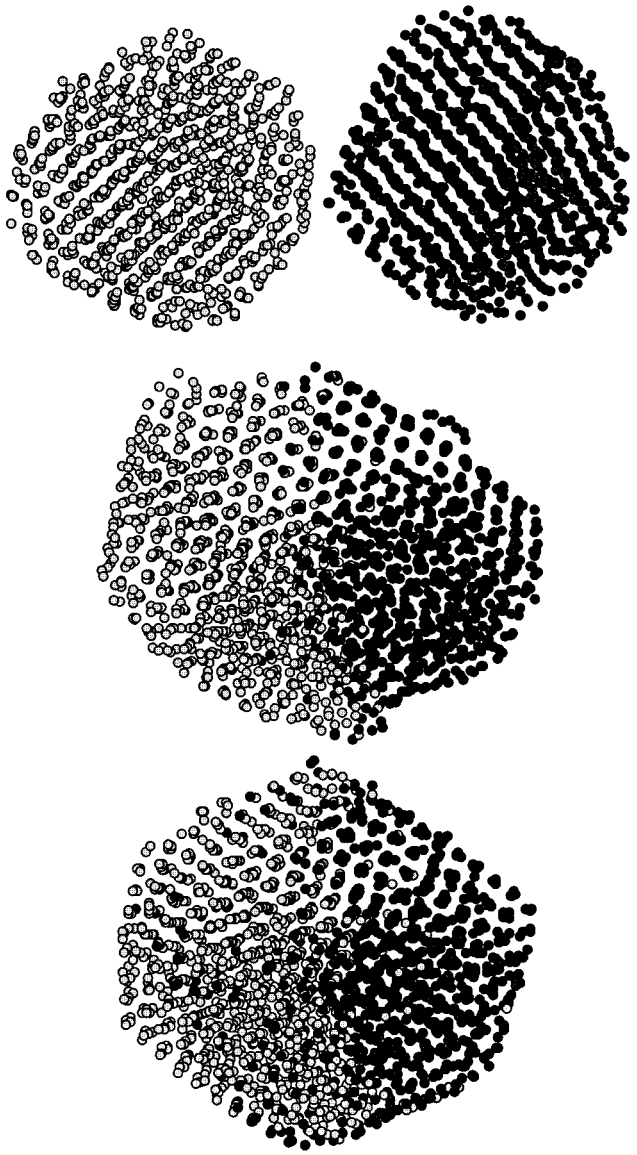

FIG. 14. Configuration of the 1055–1055 solid-solid system at three different times: 0, 1 ns, and 10 ns (top to bottom).

ing from Fig. 11 we see that the internal structure of the 767–1505-atom cluster is complex and perhaps ''grainy,'' i.e., consisting of grains or domains. Thus there are high-energy extended defects, or grain boundaries, that prevent crystallization into a single domain from taking place. In contrast, for the 1055–1055-atom system, we seem to have more of a single-domain structure. Thus the coalescence of two solid clusters is expected to depend strongly on the ''initial conditions,'' i.e., relative orientations, while this should not be the case for the coalescence of a liquid and a solid, though misfits might develop.

V. CONCLUDING REMARKS

In this paper, we have presented a MD-EAM study of some dynamic and thermodynamic properties of unsupported gold nanoparticles. With regards to thermodynamics, we focused on the melting transition of small (less than 3 nm) clusters. Our results are consistent with those reported in Refs. 7 and 6, using a many-body ''glue'' Hamiltonian. In particular, we observe that melting proceeds from the surface inwards, i.e., there exists a dynamical ''premelting'' of the outer layers signaling the approach of the melting point. A noteworthy result of our simulations is the evidence for a large (a few hundred K) melting hysteresis for the clusters, in qualitative agreement with experiments on lead.[19]

As in earlier experimental or numerical work, the analysis of the melting-freezing cycle raises questions on the applicability of macroscopic concepts—such as crystal, liquid, and surface tension—to clusters consisting of more than a hundred atoms or so. We find, in particular, that the deviation of the melting temperature from the bulk value is reasonably well described in terms of such concepts. Clearly, however, the clusters exhibit polymorphism and structural transitions that are not taken into account in this microscopic approach (see Fig. 2), but these aspects do not seem to be essential when the number of atoms exceeds a few hundred.

This situation for the melting-freezing transition is in sharp contrast with our findings for cluster coalescence. Here the macroscopic theories of sintering via surface diffusion completely fail, both qualitatively and quantitatively, to describe the coalescing behavior of two small clusters. We attribute this failure to the fact that the nanocrystals are faceted, while the sintering theories are formulated for macroscopically smooth crystallites. In order to attain the spherical equilibrium shape that can be expected from thermodynamic considerations, a cluster has to reduce the number of its facets. Such a process, in turn, requires collective rearrangement of the atoms, with correspondingly high-energy barriers. To our knowledge, the difficult problem of the approach to equilibrium of a faceted crystal has not, up to now, been investigated theoretically.

The fact that the coalescence process is ''slow,'' or slower than expected, has important consequences for the morphology of cluster-assembled materials. Indeed, the type of morphology—compact or ramified—depends critically on the ratio between the coalescence time and the time it takes for a new cluster to join an existing group.[11] If this ratio is larger than 1, ramified objects are expected to form, as observed, for instance, in Ref. 11. In the opposite case, compact objects will result, and the material will be unable to retain memory of the initial ''building blocks'' from which it was formed, thus leading to a smooth, uniform structure. It is therefore important to study further coalescence in order to characterize such effects in more detail.

ACKNOWLEDGMENTS

It is a pleasure to thank R. Kofman (Université de Nice) and P. Mélinon (UCBL) for many useful discussions. L.J.L. is thankful to Professor Serughetti and Professor Barrat for the invitation at the DPM/UCBL, where most of the work presented here was carried out, as well as the personnel of the laboratory for their kind hospitality; financial support from the CNRS is also gratefully acknowledged. This work was also supported by the Pôle Scientifique de Modélisation Numérique at ENS-Lyon, the Natural Sciences and Engineering Research Council of Canada, and the ''Fonds pour la formation de chercheurs et l'aide à la recherche'' of the Province of Québec.

*Corresponding author. Permanent address: Département de Physique, Université de Montréal, Case Postale 6128, Succursale Centre-Ville, Montréal, Québec, Canada H3C 3J7. Electronic address: lewis@physcn.umontreal.ca

[1] See, for instance, P. Mélinon, V. Paillard, V. Dupuis, A. Perez, P. Jensen, A. Hoareau, J. P. Perez, J. Tuaillon, M. Broyer, J. L. Vialle, M. Pellarin, B. Baguenard, and J. Lerme, Int. J. Mod. Phys. B **9**, 339 (1995), and references therein.

[2] See for instance, W. D. Luedtke and U. Landman, J. Phys. Chem. **100**, 13 (1996); **100**, 323 (1996); O. H. Nielsen, J.-P. Sethna, P. Stoltze, K. W. Jacobsen, and J. K. Nørskov, Europhys. Lett. **26**, 51 (1994).

[3] See, for instance, U. Röthlisberger, W. Andreoni, and M. Parrinello, Phys. Rev. Lett. **72**, 665 (1994); J. C. Charlier, A. DeVita, X. Blase, and R. Car Science **275**, 646 (1997).

[4] M. Flüelli, P. A. Buffat, and J.-P. Borel, Surf. Sci. **202**, 343 (1988).

[5] Ph. Buffat and J.-P. Borel, Phys. Rev. A **13**, 2287 (1976); J.-P. Borel, Surf. Sci. **106**, 1 (1981).

[6] X. Yu and P. M. Duxbury, Phys. Rev. B **52**, 2102 (1995).

[7] F. Ercolessi, W. Andreoni, and E. Tosatti, Phys. Rev. Lett. **66**, 911 (1991).

[8] P. Labastie and R. L. Whetten, Phys. Rev. Lett. **65**, 1567 (1990).

[9] F. Celestini, R. J.-M. Pellenq, P. Bordarier, and B. Rousseau, Z. Phys. D **37**, 49 (1996).

[10] A. Perez, P. Mélinon, V. Dupuis, P. Jensen, B. Prevel, J. Tuaillon, L. Bardotti, C. Martet, M. Treilleux, M. Broyer, M. Pellarin, J. L. Vialle, and B. Palpant, J. Phys. D **30**, 1 (1997).

[11] L. Bardotti, P. Jensen, A. Hoareau, M. Treilleux, and B. Cabaud, Phys. Rev. Lett. **74**, 4694 (1995); Surf. Sci. **367**, 276 (1996).

[12] P. Deltour, P. Jensen, and J.-L. Barrat, Phys. Rev. Lett. **78**, 4597 (1997).

[13] See, for instance, D. Frenkel and B. Smit *Understanding Molecular Simulation* (Academic, New York, 1996); M. P. Allen and D. J. Tildesley, *Computer Simulation of Liquids* (Clarendon, Oxford, 1987).

[14] S. M. Foiles, M. I. Baskes, and M. S. Daw, Phys. Rev. B **33**, 7983 (1986).

[15] M. S. Daw, S. M. Foiles, and M. I. Baskes, Mater. Sci. Rep. **9**, 251 (1993); S. M. Foiles, in *Equilibrium Structure and Properties of Surfaces and Interfaces*, edited by A. Gonis and G. M. Stocks (Plenum, New York, 1992), p. 89.

[16] G. Boisvert, L. J. Lewis, M. Puska, and R. Nieminen, Phys. Rev. B **52**, 9078 (1995).

[17] Pôle Scientifique de Modélisation Numérique, École Normale Supérieure de Lyon.

[18] H. Reiss, P. Mirabel, and R. L. Whetten, J. Phys. Chem. **92**, 7241 (1988).

[19] R. Kofman, P. Cheyssac, A. Aouaj, Y. Lereah, G. Deutscher, T. Ben David, J. M. Penisson, and A. Bourret, Surf. Sci. **303**, 231 (1994).

[20] A. Zangwill, *Physics at Surfaces* (Cambridge University Press, Cambridge, 1988).

[21] S. Valkealahti and M. Manninen, Z. Phys. D (to be published).

[22] A. Stella, P. Cheyssac, and R. Kofman in *Science and Technology of Thin Films*, edited by F. C. Matacotta and G. Ottaviani (World Scientific, Singapore, 1996), Vol. 57, p. 57.

[23] H. Zhu and R. S. Averback, Philos. Mag. Lett. **73**, 27 (1996).

[24] F. A. Nichols and W. W. Mullins, J. Appl. Phys. **36**, 1826 (1965); F. A. Nichols, *ibid.* **37**, 2805 (1966).